

Published in final edited form as:

J Mater Sci Mater Med. 2012 January ; 23(1): 157–170. doi:10.1007/s10856-011-4499-9.

Using chondroitin sulfate to improve the viability and biosynthesis of chondrocytes encapsulated in interpenetrating network (IPN) hydrogels of agarose and poly(ethylene glycol) diacrylate

Ganesh C. Ingavle, Nathan H. Dormer, Stevin H. Gehrke, and Michael S. Detamore

Department of Chemical and Petroleum Engineering Learned Hall, University of Kansas, Room 4132, 1530 W. 15th Street, Lawrence, KS 66045-7609, USA

Ganesh C. Ingavle: ganesh@ku.edu; Nathan H. Dormer: nhdormer@ku.edu; Stevin H. Gehrke: shgehrke@ku.edu; Michael S. Detamore: detamore@ku.edu

Abstract

We recently introduced agarose-poly(ethylene glycol) diacrylate (PEGDA) interpenetrating network (IPN) hydrogels to cartilage tissue engineering that were able to encapsulate viable cells and provide a significant improvement in mechanical performance relative to its two constituent hydrogels. The goal of the current study was to develop a novel synthesis protocol to incorporate methacrylated chondroitin sulfate (MCS) into the IPN design hypothesized to improve cell viability and biosynthesis. The IPN was formed by encapsulating porcine chondrocytes in agarose, soaking the construct in a solution of 1:10 MCS:PEGDA, which was then photopolymerized to form a copolymer network as the second network. The IPN with incorporated CS (CS-IPN) (~0.5 wt%) resulted in a 4- to 5-fold increase in the compressive elastic modulus relative to either the PEGDA or agarose gels. After 6 weeks of *in vitro* culture, more than 50% of the encapsulated chondrocytes remained viable within the CS-modified IPN, in contrast to 35% viability observed in the unmodified. At week 6, the CS-IPN had significantly higher normalized GAG contents ($347 \pm 34 \mu\text{g}/\mu\text{g}$) than unmodified IPNs ($158 \pm 27 \mu\text{g}/\mu\text{g}$, $P < 0.05$). Overall, the approach of incorporating biopolymers such as CS from native tissue may provide favorable micro-environment and beneficial signals to cells to enhance their overall performance in IPNs.

1 Introduction

Arthritis is the leading cause of disability among Americans, and the most common form of arthritis is osteoarthritis, with 21 million Americans suffering from this degenerative condition [1]. Injury to articular cartilage is a major contributor to the onset of osteoarthritis [2, 3]. With over two million articular cartilage defects being diagnosed each year in Europe and the USA, interest in cartilage repair has escalated [4]. The clinical need for improved treatment options for patients with cartilage injuries has motivated tissue engineering studies aimed at the *in vitro* generation of cell-based replacement tissues (or implants) with two functional properties: the ability for load bearing and capacity for integration with the host tissues [5].

Hydrogels, a promising class of materials for cartilage regeneration, can be formed from or blended with cartilage extracellular matrix (ECM) components by methods such as physical

gelation, chemical crosslinking, and self-assembly [6, 7]. Among the classes of synthetic hydrogels, poly(ethylene glycol) (PEG)-based hydrogels such as PEG diacrylate (PEGDA) hydrogels have been widely investigated as synthetic scaffolds for tissue engineering [8]. They are particularly attractive because they offer a wide range of tunable physical and mechanical properties as well as incorporated biofunctionality through variations in polymerization conditions.

An interpenetrating polymer network (IPN) is a polymer comprising two or more networks that are physically interlocked on a molecular scale, but not covalently bonded to each other. Since the two networks are independent of each other, but physically enmeshed, this type of network is termed an *interpenetrating network* or IPN. In general, IPNs have properties that either retain the characteristics of the individual networks or are an average of the two independent networks [9]. A recently published study on semi-IPNs of PEG-DA and hyaluronic acid for a fibroblast application exhibited tensile moduli in the 25–50 kPa range, which would be far below the modulus required for engineered cartilage [10]. Gong, Osada and coworkers discovered that for a variety of hydrogel IPNs and semi-IPNs, the mechanical performance of the IPNs was far superior to either of the ‘parent’ networks. They reported the synthesis of IPNs and semi-IPNs of various combinations of biological and synthetic polymers with substantially improved mechanical properties [11–18]. The magnitude of the improvement of mechanical performance seen for these network combinations was far greater than previously demonstrated in prior literature on IPNs, and because properties were so dramatically improved, Gong and Osada decided to term such materials “Dual Network” (DN) gels to distinguish them from IPNs of conventional properties.

Regarding biomedical applications, Gong and Osada recognized that the properties they measured with these DNs compare favorably with biomaterials such as cartilage. Thus, they have begun studies on the potential of these DN materials for applications such as replacement of damaged cartilage. They have recently reported on cell-DN interactions and the performance of DN gels implanted subcutaneously in rabbits [19]. Frank and coworkers [20–22] reported that dual network gels of poly(ethylene oxide) (PEO) and poly(acrylic acid) (PAA) also have superior mechanical performance while showing good biocompatibility in corneal applications. Recently, Waters and coworkers [23] reported a mechanism of strength enhancement in poly(ethylene glycol) (PEG)-poly(acrylic acid) PAA IPN hydrogels. All of these attempts were focused on the importance of the mechanical performance of hydrogels in tissue engineering. However, they did not demonstrate the capability of these DN materials or polymerization conditions to successfully *encapsulate live cells* for tissue engineering, nor were their synthesis methods amenable to viable cell encapsulation.

Synthetic IPN hydrogels alone cannot provide an ideal environment to support cell adhesion and tissue formation due to their biologically inert nature. Extracellular matrix (ECM)-mimetic modification of synthetic hydrogels has emerged as an important strategy to modulate specific cellular responses. Therefore, developing an IPN biomaterial with both biological and synthetic components with ECM-mimetic modification is of significant interest. The biological molecule chondroitin sulfate (CS), a major component of human cartilage, can provide cues to stimulate cells to proliferate, migrate, differentiate and produce ECM. Chondroitin sulfate is a sulfated glycosaminoglycan (GAG) composed of a chain of alternating sugars (*N*-acetylgalactosamine and glucuronic acid). The CS component of the IPN is hypothesized to emulate the native biochemical environment of cartilage, to provide “raw material” building blocks to the cells and help promote cartilage tissue formation through increased cell proliferation and stimulated proteoglycan secretion [24, 25]. Introducing charge into the network could also increase the water content and alter the mechanical performance of the IPN gel.

There have been a number of papers published on the subject of crosslinking GAGs for biomedical use [26–34]. A good example of this approach is given by the work of Li et al. [29]. Chondroitin sulfate was functionalized with methacrylate groups, and then solutions of this polymer were mixed with PEG(3400)-DA to form 20 w/v% concentrations and photopolymerized. Bryant et al. [27] copolymerized different ratios of MCS and PEG-DA (such as 10:90, 25:75, 40:60 and 100:0% wt/wt) into copolymer networks and studied the effect of these concentrations on macroscopic properties of gels as well as biosynthesis of encapsulated chondrocytes. They observed that higher amounts of CS enhances the gel macroscopic properties, but inhibits chondrocyte biosynthetic activity, while the PEG base chemistry enhances the tissue formation that is comprised of collagen and GAG. However, these materials were copolymers, not IPNs. The use of biofunctionalized IPNs as tissue engineering scaffolds for the regeneration, as opposed to replacement, of damaged tissues has not yet been proposed. This may be because the IPNs described to date have not been synthesized under conditions suitable for maintaining viability of encapsulated cells.

Previously, we reported a novel method for encapsulating cells in interpenetrating network (IPN) hydrogels of superior mechanical performance [35]. Taking into consideration properties such as mechanical performance, long term cell survivability, and native microenvironment of scaffolds, in the present study we designed an IPN hydrogel scaffold composed of agarose and a neutral synthetic component, PEG-DA, and incorporated a low concentration of a negatively charged biological polymer, chondroitin sulfate (CS) to test the hypothesis that CS would bolster cell viability and performance.

2 Materials and methods

2.1 Materials

2-hydroxyethyl agarose (Type VII) and high purity poly(ethylene glycol) diacrylate (PEGDA) (molecular weight 2,000 Da) were obtained from Sunbio Inc. (Anyang City, South Korea). The photoinitiator, 2-hydroxy-1-[4-(2-hydroxyethoxy)phenyl] 2-methyl-1-propanone (Irgacure 2959), was purchased from Ciba Specialty Chemicals Corp. (New York, NY). Chondroitin sulfate A sodium salt (CS) (Type A 70%, balanced with Type C, from bovine trachea; Sigma, St. Louis, MO) was used as received. Glycidyl methacrylate (97.0% purity) was purchased from Sigma-Aldrich Chemical Co. (Milwaukee, WI) and also used as received.

2.2 Bio-macromer synthesis

Chondroitin sulfate A sodium salt (CS) was methacrylated using methods adapted from Li et al. [29]. Briefly, 5 g of CS was dissolved in 50 ml of phosphate buffered saline (PBS). 5 ml of glycidyl methacrylate (GMA) was added to the CS solution and the reaction was stirred at room temperature for 15 days. Next, methacrylated chondroitin sulfate (MCS) was precipitated in acetone (1:20 v/v), then filtered and re-dissolved in 100 ml of Milli-Q water followed by chloroform extraction (1:1 v/v). The aqueous polymer solution was separated from the chloroform via a separatory funnel and concentrated back to about 50 ml by rotavap, followed by a second acetone precipitation (1:20 v/v), centrifugation, and acetone removal. Acetone was removed by drying in air at room temperature. The resulting precipitant was collected and dried at room temperature for 48 h. The MCS was re-dissolved in water and lyophilized (-46°C , 0.0140 mBar).

^1H nuclear magnetic resonance (NMR) was performed on the dried sample to quantify degree of methacrylation. High-resolution, ^1H NMR spectra were taken on a AV500 NMR spectrometer operating at 500 MHz. Deuterated water (90% D_2O + 10% H_2O) was used as the solvent, and the macromer concentrations were varied between 2.5 and 3 wt%. The ratio of

the average integrated region of the double bond proton to the integrated region of the anomeric proton of CS was used to calculate the degree of substitution (DS) of the methacrylate (MA) per repeating unit on MCS.

2.3 Synthesis of the agarose network

Briefly, 0.3 g agarose powder was added to 10 ml of PBS (pH = 7.4, 0.01 M) and autoclaved for 30 min. Once the agarose cooled to 39°C, it was combined in a 2:1 ratio with PBS to yield a 2% w/v agarose solution, and then pipetted into disk-shaped molds formed from a 1.9 mm thick silicone rubber gasket with 5 mm diameter circles punched out and sandwiched between glass plates. After cooling the molds at 4°C for 10 min, the gels were removed and added to a reservoir of PBS. Gels were allowed to equilibrate in PBS for at least 24 h before use.

2.4 Synthesis of a bio-functionalized MCS-PEGDA network and the IPN

A solution of 0.1% w/v Irgacure-2959 photoinitiator in deionized water (DI) was dissolved in a 15% w/v solution of MCS and PEGDA (1:10 mass ratio) in PBS at room temperature. For each ml of monomer solution, one agarose gel disk, prepared as described above, was added and soaked under constant agitation using a rocker for 2.5 h to achieve equilibrium. Afterward, the equilibrated gels were placed in rectangular silicon molds between optical glass microscope slides (1 mm thick), and the surrounding volume was filled with excess MCS-PEGDA/PBS solution from the soak vials. The gels were exposed to ultraviolet light for 5 min on each side using 312 nm light, 3.0 mW/cm² (Spectrolinker XL-100; Spectronics Corp.). Similarly, pure PEG-DA and IPN networks in the absence of CS were synthesized using our previously described procedure [35]. Using a 2 mm biopsy punch, gels were then cut from both the pure CS-PEGDA area and the CS-IPN area and added to excess PBS. Gels having 2 mm diameter and 2 mm height were allowed to equilibrate in PBS and deionized (DI) water for at least 24 h before use. A two-step process was selected for synthesis of IPN gel because agarose and PEGDA will otherwise phase separate if blended prior to polymerization.

2.5 Swelling degree and chemical composition of gels

Solid content was analyzed to quantify the final polymer content in each of the hydrogel groups. Gels were placed in excess DI water for at least 24 h to remove extractable materials from polymer networks and to swell to equilibrium. Equilibrated gel samples were weighed and placed into a desiccation chamber over calcium sulfate at room temperature. After at least 48 h, the dried gel samples were removed and weighed again. The solid fraction is simply the ratio of the dry mass to wet mass, and its mathematical inverse is the mass swelling degree, *Q*. The final content of agarose and PEGDA in the IPN were determined using solid content analysis, while incorporated CS content was calculated on the basis of biochemical (GAG) analysis.

2.6 Chondrocyte isolation and culture

Articular cartilage samples were dissected aseptically from ankles of 8–9 month old male Duroc hogs, which were obtained from a local butcher. Cells were harvested within 36 h after slaughter following aseptic procedures in our recent reports [36, 37]. The articular cartilage samples were diced into approximate 1 mm³ pieces using a scalpel in autoclaved PBS. After rinsing with PBS three times, the cartilage samples were digested in a sterile filtered solution of 30 ml of 2 mg/ml type II collagenase (305 U/mg; Worthington Biochemical) for 18 h on an orbital shaker in a humidified 37°C, 5% CO₂ incubator. The digested cartilage solution was filtered through a 100 µm filter cell strainer to remove undigested cartilage lumps. The filtrate was then centrifuged at 1,500 rpm for 5 min, and

then the cell pellet was resuspended in chondrocyte culture medium in a humidified incubator (37°C, 5% CO₂). The culture medium consisted of Dulbecco's modified Eagle's medium (DMEM) with 4.5 g/l D-glucose supplemented with 10% fetal bovine serum (FBS), 1% nonessential amino acids, 1% sodium pyruvate, 50 µg/ml ascorbic acid and 0.25 mg/ml penicillin-streptomycin fungicide. The DMEM and supplements were obtained from Invitrogen (Grass Islands, NY). Cell number was determined using a hemocytometer. The freshly isolated cells were grown to 90–95% confluence in T75 flasks and then retrieved by trypsin-ethylene-diaminetetraacetic acid (EDTA) digestion. First passage chondrocytes were used in this study. Culture medium was changed every 2 or 3 days.

2.7 Encapsulation of chondrocytes into CS-incorporated IPN

Chondrocytes were encapsulated in CS-incorporated IPNs using our previously published methods [35]. The chondrocytes were detached from T75 flasks using trypsin-EDTA and resuspended in PBS at a high concentration, while an agarose solution was prepared by adding 0.3 g agarose powder (cell culture grade) to 10 ml PBS and autoclaving for 30 min. The agarose solution temperature was monitored under an aseptic environment until 39°C was reached. Cells from the PBS suspension were counted using a hemocytometer. Once the agarose solution temperature reached 39°C, the chondrocyte suspension was added to the liquid agarose in a 1:2 ratio for a final concentration of 25 million cells/ml in 2% agarose. The cell suspension was mixed thoroughly with the agarose solution and pipetted into sterilized disk-shaped molds formed from a 1.9 mm thick silicone rubber gasket with 5 mm diameter circles punched out. The molds were clamped and cooled at 4°C for 9–10 min, and then chondrocyte encapsulated agarose gel constructs were transferred to non-tissue-cultured 24-well plates. Each well was supplied with 1.5 ml of fresh growth medium, and placed in an incubator overnight.

After 24 h, chondrocyte-encapsulated agarose constructs were soaked in a sterile-filtered 15% w/v solution of photopolymerizable MCS and PEGDA macromers (1:10 mass ratio) for 2.5 h, previously shown to be adequate for equilibration with PEGDA [35]. Cellular IPN constructs were made aseptically using the same procedure as described in Sect. 2.4. Using a 3 mm biopsy punch, gel samples were then cut from the center of the IPN area. The IPN constructs with encapsulated cells were then cultured for 6 weeks at 37°C with 5% CO₂ in 1.5 ml chondrocyte growth medium (Dulbecco's modified Eagle's medium [DMEM] with 4.5 g/l D-glucose supplemented with 10% fetal bovine serum (FBS), 1% nonessential amino acids, 1% sodium pyruvate, 50 µg/ml ascorbic acid and 0.25 mg/ml penicillin-streptomycin fungicide), which was replaced every 2–3 days.

2.8 Mechanical testing (compression to failure)

The compressive modulus of the IPN hydrogels was determined at room temperature on a RSA-III dynamic mechanical analyzer (TA Instruments) and tested under unconfined uniaxial compression with a 35 N loading cell ($n=5$). The gel diameter was measured with calipers under a stereomicroscope (20× magnification) and the height was measured directly using the RSA-III. All measurements and mechanical testing were performed on IPN gels swollen to equilibrium in PBS, and compression plates were lubricated with mineral oil both to minimize any gelplate adhesion and to prevent gel drying during testing. Hydrogels were then compressed in the direction normal to the circular face of the IPN gel at a rate of 0.0005 mm/s (1.7%/min) until mechanical failure occurred (indicated by a sudden drop in the compressive force). The compressive elastic modulus, defined as the slope of the initially linear region of the stress-strain curve of a material under compression, was calculated from the initial linear portion of the curve (<20% strain). Fracture points were identified at the peak stress after which a significant (>10%) decrease in stress occurred. Shear modulus values were calculated using the neo-Hookean model for ideal elastomers. The plot of stress

versus the strain function, $\lambda - 1/\lambda^2$, where $\lambda = L/L_0$ (as suggested by neo-Hookean model), yields a straight line under ideal conditions, where the slope of the line is equal to the gel shear modulus [38]. The values were used in the calculations for a set of at least 5 samples.

2.9 Live/dead assay

To compare the viability of cells encapsulated in the CS-IPN and the pure IPN, a live/dead assay was performed immediately after 0, 3, and 6 weeks of culture ($n = 3$) using a live/dead viability cytotoxicity kit (Molecular Probes). This kit contains 2 mM Calcein-AM to stain the living cells and 4 mM ethidium homodimer-1 to stain the dead cells. Cylindrical hydrogel constructs ($n = 3$) were sectioned horizontally into two equal halves and incubated in Live/Dead reagents for 30 min before imaging to promote thorough staining. Fluorescence spinning-disk confocal microscopy was used to visualize the green living cells and the red dead cells, using a Yokogawa CSU10 spinning-disk attached to an Olympus IX 81 microscope with 488 nm excitation/515–540 nm emission and 561 nm excitation/585 LP emission filters with a charge-coupled device camera (CoolSnap HQ2; Photometrics) controlled by Slidebook software (version 4.2; Intelligent Imaging Innovations, Inc.). Z-scans were performed to 350–500 μm resolution depth in areas representative of the overall IPN gels. Images were acquired in 2×2 binning mode. The three-dimensional images were deconvoluted using a constrained iterative algorithm (Slidebook). The percentage of total viable cells was calculated using the SlideBook (version 5.0) Mask Statistic module.

2.10 Biochemical assays

Biochemical assays were performed on the CS-incorporated IPN (CS-IPN) as well as pure IPN constructs ($n = 4$). At 0, 3, and 6 weeks, four samples were removed aseptically from culture and placed in microcentrifuge tubes. Samples were mechanically crushed and then homogenized with a papain mixture [125 mg/ml papain (from papaya latex), 5 mM N-acetyl cysteine, 5 mM EDTA, and 100 mM potassium phosphate buffered saline (PBS)] and allowed to digest overnight in a 60°C water bath. All reagents were obtained from Sigma. The digested constructs were then stored at -20°C . The digested constructs were thawed in a 37°C water bath and centrifuged at 10,000 rpm for 10 min to pellet fragments of polymers before conducting assays. Supernatant was used to determine GAG, DNA, and collagen content. DNA content was quantified using the Picogreen assay (Molecular probes) according to the manufacturer's instructions. Total glycosaminoglycan (GAG) content was determined using the Dimethylmethylene Blue (DMMB) (Biocolor, Carrickfergus, UK) spectrophotometric assay, with chondroitin sulfate as a standard [39]. The GAG content associated with the incorporated CS was measured using samples ($n = 4$) collected from acellular CS-IPN hydrogels (5.9 ± 3.8 $\mu\text{g}/\text{construct}$, 5.8 ± 1.7 $\mu\text{g}/\text{construct}$ and 3.9 ± 2.9 $\mu\text{g}/\text{construct}$ at 0, 3 and 6 weeks time periods, respectively). These values were subtracted from the GAG values of cellular CS-IPN samples to get the reported GAG contents for the experimental groups. As an indicator of collagen content, a hydroxyproline assay was assessed as described in our previous publication [40]. Both GAG and collagen contents were normalized to DNA content.

2.11 Histology

Histological analysis was performed using safranin O and hematoxylin & eosin (H & E) staining on cell encapsulated constructs at 0, 3, and 6 weeks ($n = 2$). Constructs were fixed in 10% formalin for 2–3 h, and soaked in optimal cutting temperature (OCT) medium [Ped Tella Inc., Redding, CA] overnight at 44°C. Constructs were then placed in a -20°C freezer until further processing. Sections were cut at -20°C using a cryostat (MICROM HM 550) to 8 μm thickness, mounted on a microscope slide and allowed to dry for 1 h at room temperature. Following standard histological procedures, the sections were stained with hematoxylin and safranin O, which stains nuclei purple and negatively charged GAGs

orange, respectively. Eosin stains cytoplasm, connective tissues and other extracellular substance red or pink.

2.12 Statistical analysis

All quantitative data were expressed as mean \pm standard deviations and were verified by single-factor analysis of variance (ANOVA) followed by Tukey's post hoc analysis. Analysis was performed using the SPSS 17.0 statistical software package. *P* values of less than 0.05 were considered statistically significant.

3 Results

3.1 CS modification and IPN synthesis

The synthesis of MCS macromer was illustrated in Fig. 1, where the epoxy rings in GMA are opened by transesterification and ring opening reactions to functionalize hydroxyl, carboxyl, and sulfate groups of chondroitin sulfate with methacrylate groups [41]. Figure 2 shows the proton NMR of the methacrylated CS with an inset of the chemical structure, which confirmed the successful grafting of the methacrylate group on CS. Two distinctive peaks, at 5.65 and 6.10 ppm, were attributed to methacrylate protons and at 5.1 ppm to anomeric protons from CS. The bioactive IPN was synthesized in this study using MCS, which was 6.3% methacrylated. The vinyl double bond on MCS reacted with PEGDA during photopolymerization in the presence of Irgacure 2959 photoinitiator and formed a poly(ethylene glycol)-CS (PEG-CS) copolymer network (Fig. 3). The synthesis of the bioactive interpenetrating network using agarose, MCS macromer, and PEGDA is shown schematically in Fig. 4.

3.2 Swelling degree and gel composition

Chondroitin sulfate (methacrylated) was incorporated into the agarose/PEG-DA IPN network by copolymerizing MCS with PEGDA after soaking agarose hydrogels in the macromer solutions, as outlined in Fig. 3 and Fig. 4. Acellular hydrogels as well as IPN constructs were characterized for their swelling behavior and solids content. The swelling degrees of various equilibrium-swollen networks are tabulated in Table 1. The final PEG-DA and PEG-CS contents in pure PEG-DA and PEG-DA-CS gels were 7.3 and 6.9%, respectively (wet basis). The solids content data in Table 1 show that agarose gels were composed of 2.4% agarose, hence by difference the PEG contents of IPN gels were estimated as 7.1% without CS and 6.4% with CS. These values were equal within experimental error to those of pure PEG and PEG-CS gels. Total CS content of the acellular CS-IPN gels, measured by the GAG assay, was 5.2 ± 2.8 $\mu\text{g}/\text{CS-IPN}$ construct ($n = 4$) or about 0.5 wt% of the total CS-IPN solid content.

The PEG and PEG-CS contents in the pure IPN and CS-IPN hydrogels were calculated by subtracting the solid contents of the pure agarose gel. CS-PEG showed an 11% greater swelling degree than the pure PEG network, but this increase in swelling degree was not statistically significant. Analogous increases were observed in the CS-incorporated IPN when compared with the normal IPN network, although these differences were not statistically significant (Table 1). Macroscopic and microscopic images of gels are displayed in Fig. 5. Equilibrium-swelled unmodified IPN and CS-incorporated IPN with encapsulated chondrocytes are shown in Fig. 5a. Figure 5b displays the homogeneous distribution of encapsulated chondrocytes within the IPN gel, while Fig. 5c displays their round morphology.

3.3 Compressive modulus

The representative stress–strain curves for the various hydrogel groups are displayed in Fig. 6. All hydrogels except agarose (because of early fracture) displayed a concave upward curve characteristic of elastomeric materials with large deformation before fracture. The Young's modulus (E) and shear modulus (G) were calculated from the slope of the initial linear neo-Hookean region of the stress–strain (<20% strain) curves (Fig. 7). Mechanical property data of all gels are summarized in Table 1. Ideal elastomers have E/G ratios of 3, although compression tests on hydrogels typically give values somewhat above 3 [42]. In Table 1, the E/G ratios average 3.6 and do not vary significantly among networks, indicating that all gels and IPNs behave as ideal elastomers and in agreement with our previously reported work on agarose-PEG IPNs [35]. The compressive shear modulus for the equilibrium swelled CS-IPN gel was 45.4 ± 7.5 kPa, while for the unmodified IPN it was 37.9 ± 9.3 kPa (Table 1). Shear moduli for acellular IPN gels were 3.7 times higher than for pure PEGDA and 4.8 times higher than pure agarose gels ($P < 0.05$), while the shear modulus of the CS-IPN group was 4.4 times higher than for the pure PEG-DA gels and 5.8 times higher ($P < 0.05$) than for the pure agarose gels (Fig. 8). Similar increases in the Young's modulus were observed (see Table 1). As far as failure properties were concerned, IPN networks were 2.5 times stronger and 3.2 times tougher than pure PEG networks, while CS-IPN networks were 2.8 times stronger and 3.6 times tougher than pure PEG networks ($P < 0.05$) (Table 1). Failure of pure CS-PEG copolymer networks occurred at lower strain than pure PEG networks and they shattered into small fragments. Similarly, CS-incorporated IPN networks were shattered into extremely small fragments (~85% strain) before unmodified IPN networks.

3.4 Cell viability

A live/dead assay was used to determine the cell viability at different time intervals after the encapsulation (Fig. 9). When compared with the incubation time periods of 0, 3 and 6 weeks, live–dead (Calcein-ethidium dye) cell staining indicated that the majority of cells encapsulated in CS-incorporated IPN hydrogels remained viable (stained fluorescent green with Calcein) over the culture period of 6 weeks (Fig. 9). The viability of chondrocytes in unmodified Agarose/PEGDA IPN hydrogels is high, but less than desirable. Mask statistics analysis showed that, in the absence of any biomolecules, viability drops to 45.3 ± 2.7 and $35.7 \pm 4.5\%$ at 3 and 6 weeks post-encapsulation in culture, respectively, while, by incorporating chondroitin sulfate within the IPN, the viability was 70.2 ± 10.3 and $55.6 \pm 14.8\%$ at 3 and 6 weeks, respectively (Fig. 10). These values were statistically significant from 0 week time point values ($P < 0.05$).

3.5 Total GAG and collagen production

DNA content analysis indicated that the resulting number of encapsulated cells in the IPNs with CS was similar to that of the unmodified IPN control at week 0, suggesting comparable cell seeding efficiencies in both unmodified as well as CS-IPN. A significant increase in DNA content was observed in both the IPN control group as well as in CS-IPN group between 0 and 6 weeks ($P < 0.05$), while it did not change significantly between 3 and 6 weeks (Fig. 11). DNA content decreased in CS-IPN as compared to the unmodified IPN group at 6 weeks.

Values from quantitative GAG analysis were determined and presented in Fig. 12. Both CS-IPN as well as unmodified IPN constructs accumulated sulfated GAGs over the 6-week culture period. GAG content per construct (gel) was noted to increase significantly over time ($P < 0.05$) and no significant differences were observed between unmodified IPN and CS-IPN at 3 and 6 weeks (Fig. 12a). Total accumulated GAG content normalized to total DNA content is presented in Fig. 12b. For GAG content calculation, the GAG value of

acellular Ag/CS-PEGDA IPN hydrogels (GAG produced by incorporated CS) was subtracted from the total value. Normalized GAG content at week 0 was different between the unmodified IPN and CS-IPN gel groups, however the difference was not statistically significant. The normalized GAG contents for all groups increased over time ($P < 0.05$, $n = 4$) and significant differences were observed between the unmodified IPN and CS-IPN at the week 6 culture period. At week 3 and week 6, the CS-IPN had significantly higher normalized GAG contents (242 ± 129 and 347 ± 34 $\mu\text{g}/\text{lg}$) than control IPNs (86 ± 13 and 158 ± 27 $\mu\text{g}/\mu\text{g}$). Results from the quantitative analysis of collagen (by hydroxylproline assay) are presented in Fig. 13. Similar to GAG, collagen per construct (gel) increased significantly ($P < 0.05$) in both of the groups from 0 to 6 weeks (Fig. 13a). Normalized collagen content increased significantly in unmodified IPN and CS-IPN hydrogels from week 0 (7.6 ± 3.6 and 9.8 ± 7.0 $\mu\text{g}/\mu\text{g}$) to week 6 (18 ± 3 and 22 ± 13 $\mu\text{g}/\mu\text{g}$) ($P < 0.05$, $n = 4$), while no significant differences were observed between unmodified IPN and CS-IPN groups at 0, 3, and 6 weeks (Fig. 13b).

3.6 Histological evaluation

Histological images of chondrocytes photoencapsulated in unmodified IPN and CS-IPN gels are shown in Fig. 14. GAG production by chondrocytes in the IPN and CS-incorporated IPN hydrogels was examined using safranin O. Intracellular staining was observed in IPN gels without CS (Fig. 14a), while the encapsulated chondrocytes in CS-IPN hydrogels exhibited dense staining in pericellular and interterritorial region (Fig. 14b). H & E staining exhibited homogeneous cell distribution and size in both the unmodified IPN group (Fig. 14c) and the CS-incorporated IPN group (Fig. 14d). Encapsulated chondrocytes in IPN gels without CS displayed the normal rounded morphology (Fig. 14c), while they showed larger diameter pericellular matrices (Fig. 14d) in CS-IPNs at week 6.

4 Discussion

Designing tissue engineering scaffolds for cartilage tissue regeneration with the required mechanical properties and favorable microenvironment to promote cell attachment, growth, and new tissue formation is one of the key challenges facing the tissue engineering field. Previously in our laboratory, we investigated agarose-poly(ethylene glycol)-based interpenetrating network (IPN) hydrogels that exhibited cytocompatibility and improved mechanical properties relative to its component networks [35]. In the current study, we focused on investigating ECM mimetic microenvironments, essential for promoting cell growth and biosynthesis in IPNs along with improved mechanical properties. To introduce CS, a natural component of cartilage, into the IPN, methacrylate groups were grafted onto CS, whereas the vinyl groups proceeded to a photopolymerization with PEG-DA. We used glycidyl methacrylate (GMA) to add methacrylate groups to CS because of the efficiency of the reaction [43, 44] and the lack of toxic byproducts.

Two properties that are particularly important for cartilage tissue engineering are the equilibrium water content (swelling degree, Q) and the compressive modulus. Since CS has a high charge density, at high incorporation levels it could lead to increased swelling of the network. In this work, because the CS incorporation level was low (~ 0.5 wt%), the PEG-CS network swelled a statistically insignificant amount more than the pure PEG-DA. The lower percentage of PEG-CS measured by solid content analysis as compared to pure PEG in the final CS-IPN may be associated with the insufficient diffusion time during soaking. The PEG-CS gels in DI water swelled to about double in size compared to pure PEG-DA hydrogels and IPNs without CS, respectively, while in phosphate buffered saline (PBS) they swelled less than other groups because the counter ions in the buffer solutions suppress swelling due to Donnan ion exclusion effects [45, 46]. The second factor that contributed to an increase in the swelling degree was the methacrylate groups on the CS.

Compressive mechanical properties are very important to develop a 3D cell-seeded scaffold for load bearing applications. We have shown previously that the IPN shear modulus is much greater than the additive sum of PEG and agarose shear moduli and the effect is also seen in the CS-IPN [35]. Mechanical failure is dependent upon both fundamental material properties as well as macro- and microscopic structural defects in particular samples. Stress-strain curves increase exponentially after 50% strain as shown in Fig. 6, and therefore sharp increase and irregular failure of these IPN gels at high strain leads to much larger standard deviations in failure stress and gel toughness. Previously, we have shown that the presence of encapsulated cells did not significantly compromise mechanical properties of this kind of IPN hydrogel [35]. This enhanced mechanical strength with good water absorption properties, induced by covalent crosslinking of CS and secondary interactions due to ionic species, allows potential use of this kind of IPN scaffold in cartilage repairs that are not possible with IPN systems containing only PEG networks. No significant differences were observed in failure strains between CS-IPN, CS-PEG, and PEG groups, and we therefore conclude that the CS-IPN represented a significant enhancement in total energy absorbed at failure by enhancing compressive shear modulus while maintaining a comparable failure strain. Increase in average fracture stress as well as toughness of CS-PEG and CS-IPN over their counterpart such as pure PEG and IPN without CS also support this conclusion.

In our previous report, we demonstrated that this IPN synthesis method was compatible with the incorporation of chondrocytes, but chondrocytes did not remain viable over time (after 1 week) when cultured [35]. In the current study, the results of the live/dead assay suggested that significantly more cells stayed alive after 6 weeks when encapsulated in the CS-incorporated IPN (CS-IPN) hydrogel as compared to the IPNs without CS. We speculate that pure IPN hydrogels, due to their bio-inert nature, lack the biological motifs to support the long-term survival of cells. To promote cellular functions, it is highly desirable that the scaffolds have cell specific adhesion and the ability to carry signaling biomolecules. Crosslinked CS molecules with PEG networks in the IPN provide a host tissue mimetic microenvironment in which cells grow and proliferate.

We observed significant differences in the production and retention of newly synthesized ECM components within unmodified IPN and CS-incorporated IPNs. As expected, there was almost no GAG production at week 0 in the pure IPN, while CS-incorporated IPN showed little GAG accumulation due to linked CS. CS-IPN accumulated significantly more GAG and collagen content than pure IPN gels at the week 3 and week 6 culture periods. In short, biosynthesis was significantly influenced by the incorporation of CS into IPN gels. The precise role of CS in enhancing GAG as well as collagen production is unclear, however these findings are supported by the previous studies that demonstrated that ECM production in cell-encapsulated PEG hydrogel scaffolds is highly dependent upon the surrounding tissuespecific microenvironment and that the presence of CS promotes biosynthesis [27, 47]. Elisseff and co-workers encapsulated chondrocytes in poly(ethylene oxide)-dimethacrylate and poly(ethylene glycol) semi-IPNs; biomechanical analysis demonstrated the presence of a functional extracellular matrix and that equilibrium moduli increased with time [9]. Our results showed CS-incorporated agarose-PEG IPNs had superior biochemical properties compared to the previously studied IPNs.

Histological evaluation supported the proper role of CS-incorporated IPN in cartilaginous tissue formation. The encapsulated cells retained a round morphology in IPN, while large irregular regions of cartilage-like tissue were observed in the CS-incorporated IPN after the 6-week culture period. Due to the presence of CS in the CS-IPN, the entire construct stained positive with Safranin O at week 6. Denser Safranin O staining at 6 weeks indicated higher GAG accumulation in CS containing IPN hydrogels compared to pure IPN hydrogels. Cells secreted proteoglycans in both the pericellular and the intercellular space throughout the

entire CS-IPN scaffold, confirming the ability of CS-IPN constructs to produce large amounts of ECM, which is essential for successful regeneration of cartilage-like tissue. In addition, the larger diameter of the pericellular matrix of encapsulated chondrocytes in CS-incorporated IPN gels by H & E staining confirmed the higher rate of matrix accumulation.

In summary, we have shown that the physical and biochemical properties of interpenetrating network (IPN) hydrogels are directly influenced by ECM-mimetic modification with chondroitin sulfate. Agarose-PEG IPN gels with a CS mediated microenvironment create a desirable 3D porous scaffold for cell encapsulation with improved mechanical properties. This cell recognizable microenvironment enables encapsulated chondrocytes to secrete and distribute ECM components when the degradation is properly tuned. It is possible to degrade a CS-PEG network by cellular secretion of the enzyme chondroitinase in a cell culture [47] and an agarose network hydrolytically [48], so a CS-IPN implant can likely be optimized for in vivo degradation.

Further studies are underway to examine whether the incorporation of other biomolecules will further improve mechanical properties, cell viability, and biosynthesis in these bio-functionalized IPN scaffolds. Future directions will focus on exploring different PEG-DA molecular weights and concentrations, as well as different ratios of chondroitin sulfate to PEG-DA.

5 Conclusions

Cartilage repair remains a challenging task due to the biological complexity of the regenerative process. Poor mechanical performance and poor cell recognizable tissue-specific microenvironments found in most synthetic hydrogels limit their application in cartilage defect repair. In this study, we successfully designed and synthesized a promising new class of *bio-functionalized* engineered IPN hydrogel scaffolds with a unique combination of high mechanical strength and cytocompatibility for the first time in cartilage tissue engineering. It was shown that the incorporation of chondroitin sulfate into a ductile PEG network created an ECM-mimetic IPN with a synergistically greater compressive modulus (relative to PEG and agarose single networks), higher swelling ratio, and improved cell response. Furthermore, these ECM-mimetic IPN gels exhibited long-term encapsulated cell viability with enhanced matrix production. There has been a growing interest in developing innovative biomaterials with improved bio-functionality (cell recognition signals) that can be used for cartilage tissue engineering. The method introduced in this study may provide a platform for developing suitable engineered scaffolds for cartilage regeneration that provide not only a superior mechanical performance, but also harness a biological cue to promote new tissue growth for cartilage defect repair.

Acknowledgments

The authors would like to thank Dr. David Moore and Heather Shinogle for their assistance during LIVE/DEAD imaging with spinning disc confocal microscopy. This work was supported by a grant from the National Institutes of Health (R21 EB008783).

References

1. Buckwalter JA, Saltzman C, Brown T. The impact of osteoarthritis: implications for research. Clin Orthop Relat Res. 2004; 427(Supp 1):S6–S15. [PubMed: 15480076]
2. D’Lima DD, Hashimoto S, Chen PC, Colwell CW Jr, Lotz MK. Impact of mechanical trauma on matrix and cells. Clin Orthop Relat Res. 2001; 391(Supp 1):S90–S99. [PubMed: 11603728]

3. Thambyah A. A hypothesis matrix for studying biomechanical factors associated with the initiation and progression of post-traumatic osteoarthritis. *Med Hypotheses*. 2005; 64(6):1157–1161. [PubMed: 15823707]
4. Reginster JY. The prevalence and burden of arthritis. *Rheumatology (Oxford)*. 2002; 41(Suppl 1):3–6. [PubMed: 12173279]
5. Butler DL, Goldstein SA, Guilak F. Functional tissue engineering: the role of biomechanics. *J Biomech Eng*. 2000; 122(6):570–575. [PubMed: 11192376]
6. Vinatier C, Guicheux J, Daculsi G, Layrolle P, Weiss P. Cartilage and bone tissue engineering using hydrogels. *Biomed Mater Eng*. 2006; 16(4 Suppl 1):S107–S113. [PubMed: 16823101]
7. Van Tomme SR, Storm G, Hennink WE. In situ gelling hydrogels for pharmaceutical and biomedical applications. *Int J Pharm*. 2008; 355(1–2):1–18. [PubMed: 18343058]
8. Peppas NA, Hilt JZ, Khademhosseini A, Langer R. Hydrogels in biology and medicine: from molecular principles to bionano-technology. *Adv Mater*. 2006; 18(11):1345–1360.
9. Elisseff J, McIntosh W, Anseth K, Riley S, Ragan P, Langer R. Photoencapsulation of chondrocytes in poly(ethylene oxide)-based semi-interpenetrating networks. *J Biomed Mater Res*. 2000; 51(2):164–171. [PubMed: 10825215]
10. Kutty JK, Cho E, Soo Lee J, Vyavahare NR, Webb K. The effect of hyaluronic acid incorporation on fibroblast spreading and proliferation within PEG-diacrylate based semi-interpenetrating networks. *Biomaterials*. 2007; 28(33):4928–4938. [PubMed: 17720239]
11. Gong JP, Katsuyama Y, Kurokawa T, Osada Y. Double-network hydrogels with extremely high mechanical strength. *Adv Mater*. 2003; 15:1155–1158.
12. Huang M, Furukawa H, Tanaka Y, Nakajima T, Osada Y, Gong JP. Importance of entanglement between first and second components in high-strength double network gels. *Macromolecules*. 2007; 40:6658–6664.
13. Kaneko D, Tada T, Kurokawa T, Gong JP, Osada Y. Mechanically strong hydrogels with ultra-low frictional coefficients. *Adv Mater*. 2005; 17:535–538.
14. Na YH, Kurokawa T, Katsuyama Y, Tsukeshiba H, Gong JP, Osada Y, Okabe S, Karino T, Shibayama M. Structural characteristics of double network gels with extremely high mechanical strength. *Macromolecules*. 2004; 37:5370–5374.
15. Nakayama A, Kakugo A, Gong JP, Osada Y, Takai M, Erata T, Kawano S. High mechanical strength double-network hydrogel with bacterial cellulose. *Adv Funct Mater*. 2004; 14:1124–1128.
16. Tanaka Y, Kuwabara R, Na YH, Kurokawa T, Gong JP, Osada Y. Determination of fracture energy of high strength double network hydrogels. *J Phys Chem B*. 2005; 109(23):11559–11562. [PubMed: 16852418]
17. Tsukeshiba H, Huang M, Na YH, Kurokawa T, Kuwabara R, Tanaka Y, Furukawa H, Osada Y, Gong JP. Effect of polymer entanglement on the toughening of double network hydrogels. *J Phys Chem B*. 2005; 109(34):16304–16309. [PubMed: 16853073]
18. Yasuda K, Gong JP, Katsuyama Y, Nakayama A, Tanabe Y, Kondo E, Ueno M, Osada Y. Biomechanical properties of high-toughness double network hydrogels. *Biomaterials*. 2005; 26(21):4468–4475. [PubMed: 15701376]
19. Azuma C, Yasuda K, Tanabe Y, Taniguro H, Kanaya F, Nakayama A, Chen YM, Gong JP, Osada Y. Biodegradation of high-toughness double network hydrogels as potential materials for artificial cartilage. *J Biomed Mater Res A*. 2007; 81(2):373–380. [PubMed: 17117467]
20. Farooqui N, Myung D, Masek M, Dalal R, Koh W, Gupta SP, Noolandi J, Frank C, Ta CN. Histological evaluation of poly(ethylene glycol)-poly(acrylic acid) (PEG-PAA) double network hydrogel corneal implant. *Invest Ophthalmol Vis Sci*. 2005; 46 E-abstract 873.
21. Koh WG, Myung D, Ko JA, Noolandi J, Frank CW, Ta CN. Synthesis and surface modification of double network hydrogel from poly(ethylene glycol) and poly(acrylic acid). *Invest Ophthalmol Vis Sci*. 2005; 46 E-Abstract 4994.
22. Myung D, Koh W, Ko J, Noolandi J, Carrasco M, Smith A, Frank C, Ta C. Characterization of poly(ethylene glycol)-poly(-acrylic acid) (PEG-PAA) double networks designed for corneal implant applications. *Invest Ophthalmol Vis Sci*. 2005; 46 E-Abstract 5003.

23. Waters DJ, Engberg K, Parke-Houben R, Ta CN, Jackson AJ, Toney MF, Frank CW. Structure and mechanism of strength enhancement in interpenetrating polymer network hydrogels. 2011; 44:5776–5786.
24. Sechriest VF, Miao YJ, Niyibizi C, Westerhausen-Larson A, Matthew HW, Evans CH, Fu FH, Suh JK. GAG-augmented poly-saccharide hydrogel: a novel biocompatible and biodegradable material to Support chondrogenesis. *J Biomed Mater Res*. 2000; 49(4):534–541. [PubMed: 10602087]
25. van Susante JLC, Pieper J, Buma P, van Kuppevelt TH, van Beuningen H, van Der Kraan PM, Veerkamp JH, van den Berg WB, Veth RPH. Linkage of chondroitin-sulfate to type I collagen scaffolds stimulates the bioactivity of seeded chondrocytes in vitro. *Biomaterials*. 2001; 22(17): 2359–2369. [PubMed: 11511033]
26. Banu N, Tsuchiya T. Markedly different effects of hyaluronic acid and chondroitin sulfate-A on the differentiation of human articular chondrocytes in micromass and 3-D honeycomb rotation cultures. *J Biomed Mater Res A*. 2007; 80(2):257–267. [PubMed: 16941596]
27. Bryant SJ, Arthur JA, Anseth KS. Incorporation of tissue-specific molecules alters chondrocyte metabolism and gene expression in photocrosslinked hydrogels. *Acta Biomater*. 2005; 1(2):243–252. [PubMed: 16701801]
28. Gilbert ME, Kirker KR, Gray SD, Ward PD, Szakacs JG, Prestwich GD, Orlandi RR. Chondroitin sulfate hydrogel and wound healing in rabbit maxillary sinus mucosa. *Laryngoscope*. 2004; 114(8):1406–1409. [PubMed: 15280717]
29. Li Q, Williams CG, Sun DD, Wang J, Leong K, Elisseff JH. Photocrosslinkable polysaccharides based on chondroitin sulfate. *J Biomed Mater Res A*. 2004; 68(1):28–33. [PubMed: 14661246]
30. Yang SH, Chen PQ, Chen YF, Lin FH. Gelatin/chondroitin-6-sulfate copolymer scaffold for culturing human nucleus pulposus cells in vitro with production of extracellular matrix. *J Biomed Mater Res B Appl Biomater*. 2005; 74(1):488–494. [PubMed: 15912520]
31. Yang SH, Chen PQ, Chen YF, Lin FH. An in vitro study on regeneration of human nucleus pulposus by using gelatin/chondroitin-6-sulfate/hyaluronan tri-copolymer scaffold. *Artif Organs*. 2005; 29(10):806–814. [PubMed: 16185342]
32. Yu X, Bellamkonda RV. Dorsal root ganglia neurite extension is inhibited by mechanical and chondroitin sulfate-rich interfaces. *J Neurosci Res*. 2001; 66(2):303–310. [PubMed: 11592128]
33. Kirker KR, Luo Y, Nielson JH, Shelby J, Prestwich GD. Glycosaminoglycan hydrogel films as bio-interactive dressings for wound healing. *Biomaterials*. 2002; 23:3661–3671. [PubMed: 12109692]
34. Salinas CN, Anseth KS. Decorin moieties tethered into PEG networks induce chondrogenesis of human mesenchymal stem cells. *J Biomed Mater Res A*. 2008; 90:456–464. [PubMed: 18546186]
35. DeKosky BJ, Dormer NH, Ingavle GC, Roatch CH, Lomakin J, Detamore MS, Gehrke SH. Hierarchically designed agarose and poly(ethylene glycol) interpenetrating network hydrogels for cartilage tissue engineering. *Tissue Eng Part C Methods*. 2010; 16(6):1533–1542. [PubMed: 20626274]
36. Wang L, Detamore MS. Effects of growth factors and glucosamine on porcine mandibular condylar cartilage cells and hyaline cartilage cells for tissue engineering applications. *Arch Oral Biol*. 2009; 54(1):1–5. [PubMed: 18640663]
37. Wang L, Lazebnik M, Detamore MS. Hyaline cartilage cells outperform mandibular condylar cartilage cells in a TMJ fibro-cartilage tissue engineering application. *Osteoarthr Cartil*. 2009; 17(3):346–353. [PubMed: 18760638]
38. Treloar, LRG. *The physics of rubber elasticity*. Oxford: Oxford University Press; 2005.
39. Farndale RW, Buttle DJ, Barrett AJ. Improved quantitation and discrimination of sulphated glycosaminoglycans by use of dim-ethylmethylene blue. *Biochim Biophys Acta*. 1986; 883(2): 173–177. [PubMed: 3091074]
40. Wang L, Tran I, Seshareddy K, Weiss ML, Detamore MS. A comparison of human bone marrow-derived mesenchymal stem cells and human umbilical cord-derived mesenchymal stromal cells for cartilage tissue engineering. *Tissue Eng Part A*. 2009; 15(8):2259–2266. [PubMed: 19260778]
41. Li Q, Wang DA, Elisseff JH. Heterogeneous-phase reaction of glycidyl methacrylate and chondroitin sulfate: mechanism of ring-opening-transesterification competition. *Macromolecules*. 2003; 36:2556–2562.

42. Xue W, Huglin MB, Jones TGJ. Swelling and network parameters of crosslinked thermoreversible hydrogels of poly (*N*-ethyl-acrylamide). *Eur Polym J.* 2005; 41:239–248.
43. Poshusta AK, Anseth KS. Photopolymerized biomaterials for application in the temporomandibular joint. *Cells Tissues Organs.* 2001; 169(3):272–278. [PubMed: 11455123]
44. van Dijk-Wolthuis W, Franssen O, Talsma H, van Steenberghe MJ, Kettenes-van den Bosch JJ, Hennink WE. Synthesis, characterization, and polymerization of glycidyl methacrylate derivatized dextran. *Macromolecules.* 1995; 28:6317–6322.
45. Flory, PJ. Principles of polymer chemistry. Ithaca: Cornell University Press; 1953.
46. Gehrke, SH. Synthesis and properties of hydrogels used for drug delivery. In: Amidon, GL.; Lee, PI.; Topp, EM., editors. *Transport processes in pharmaceutical systems.* New York: Marcel Dekker; 2000. p. 473-546.
47. Varghese S, Hwang NS, Canver AC, Theprungsirikul P, Lin DW, Elisseeff J. Chondroitin sulfate based niches for chondrogenic differentiation of mesenchymal stem cells. *Matrix Biol.* 2008; 27(1):12–21. [PubMed: 17689060]
48. De Rosa E, Urciuolo F, Borselli C, Gerbasio D, Imparato G, Netti PA. Time and space evolution of transport properties in agarose-chondrocyte constructs. *Tissue Eng.* 2006; 12(8):2193–2201. [PubMed: 16968160]

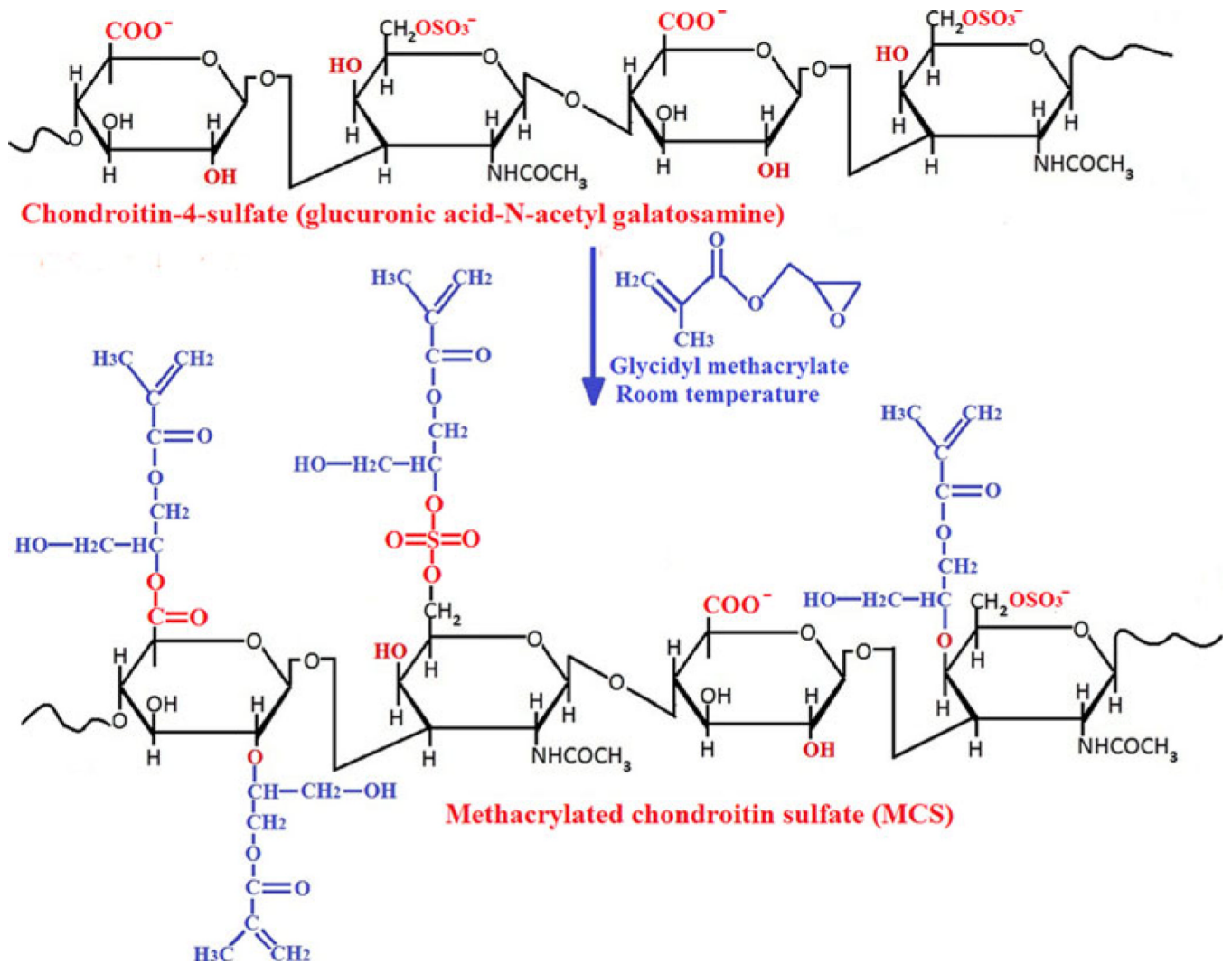


Fig. 1. Schematic representation showing the synthesis of methacrylated chondroitin sulfate (MCS) and indicating the potential sites of methacrylate functionalization of CS

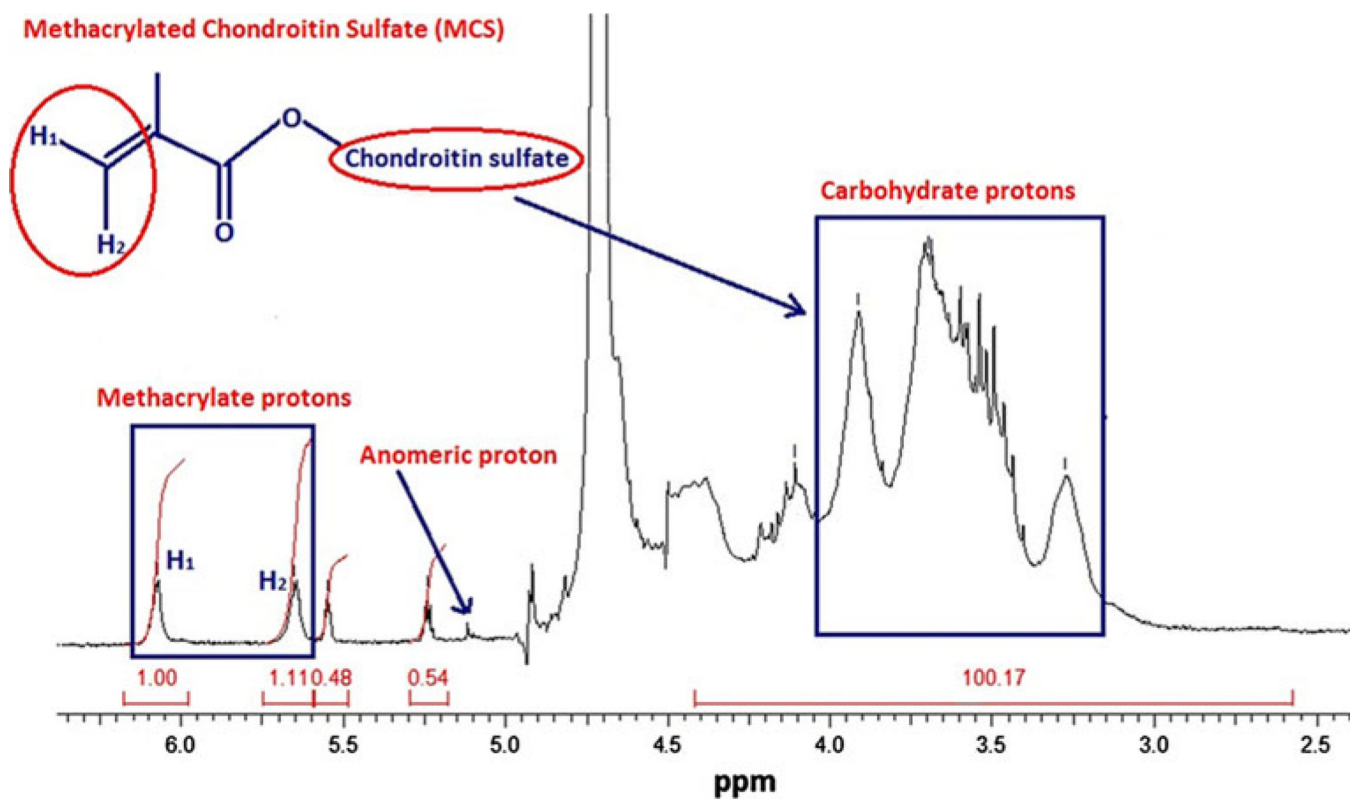


Fig. 2. Proton NMR spectra of methacrylated chondroitin sulfate (MCS)

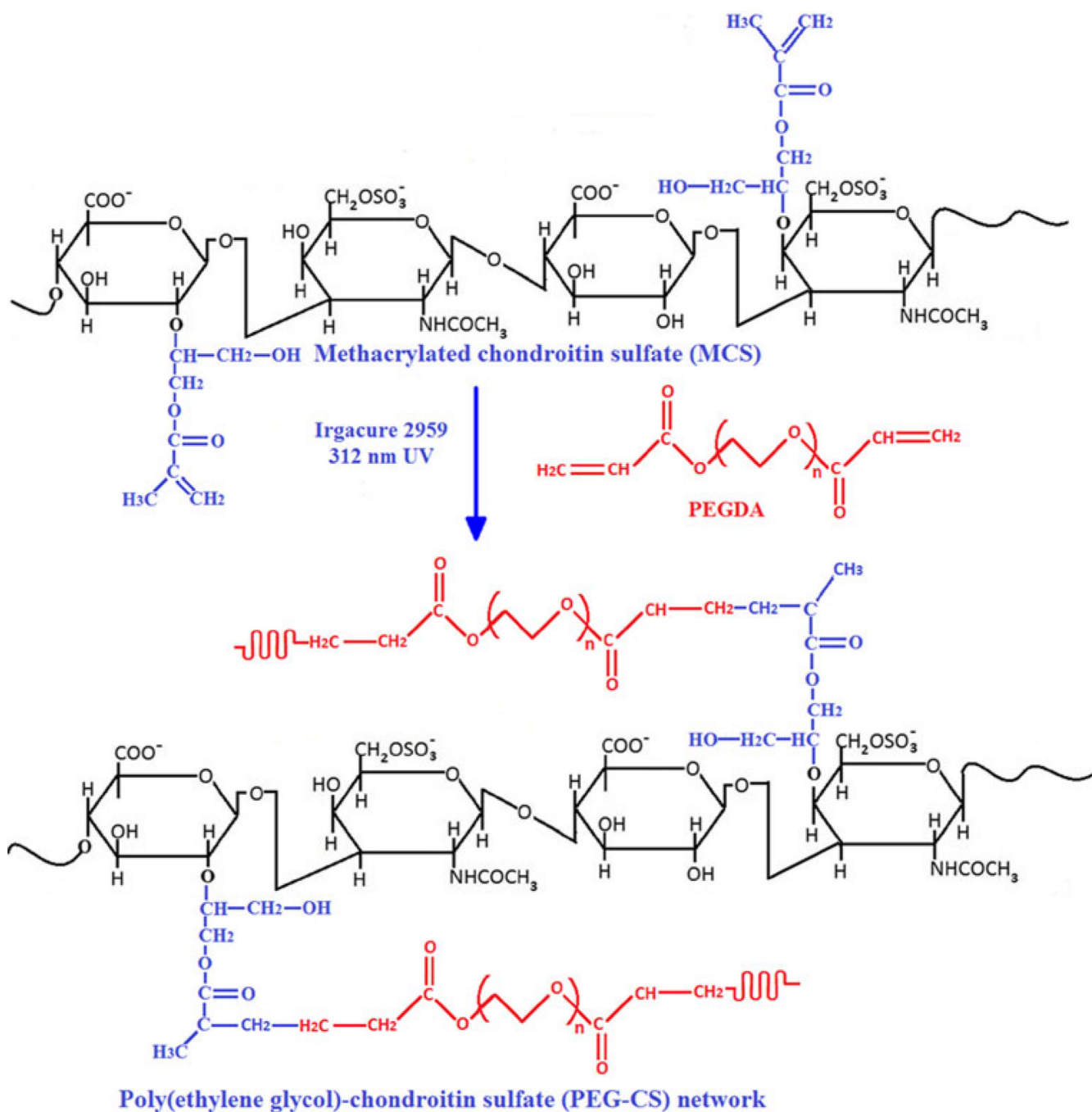


Fig. 3. Illustration of the reaction scheme for PEGDA with MCS. Note that PEG-DA can also react with itself to form a network

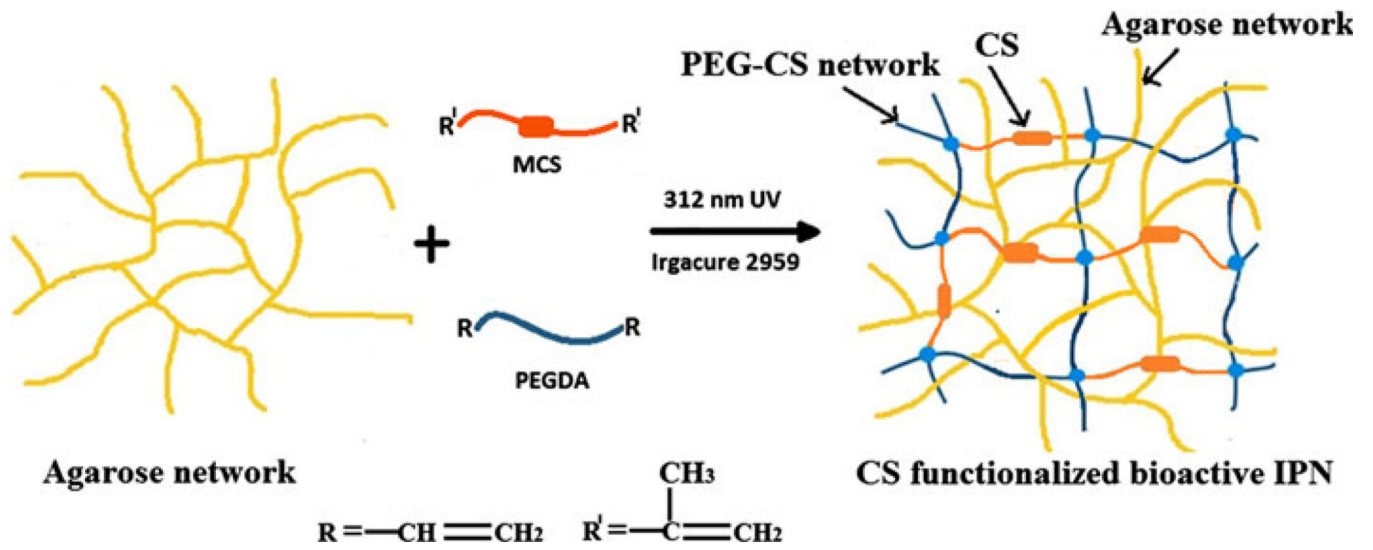


Fig. 4. Schematic diagram showing the synthesis of bio-functionalized interpenetrating network (IPN) gels with agarose as the first network interlocked with the CS-PEG network, creating a mechanically stiffer and tougher bioactive IPN gel

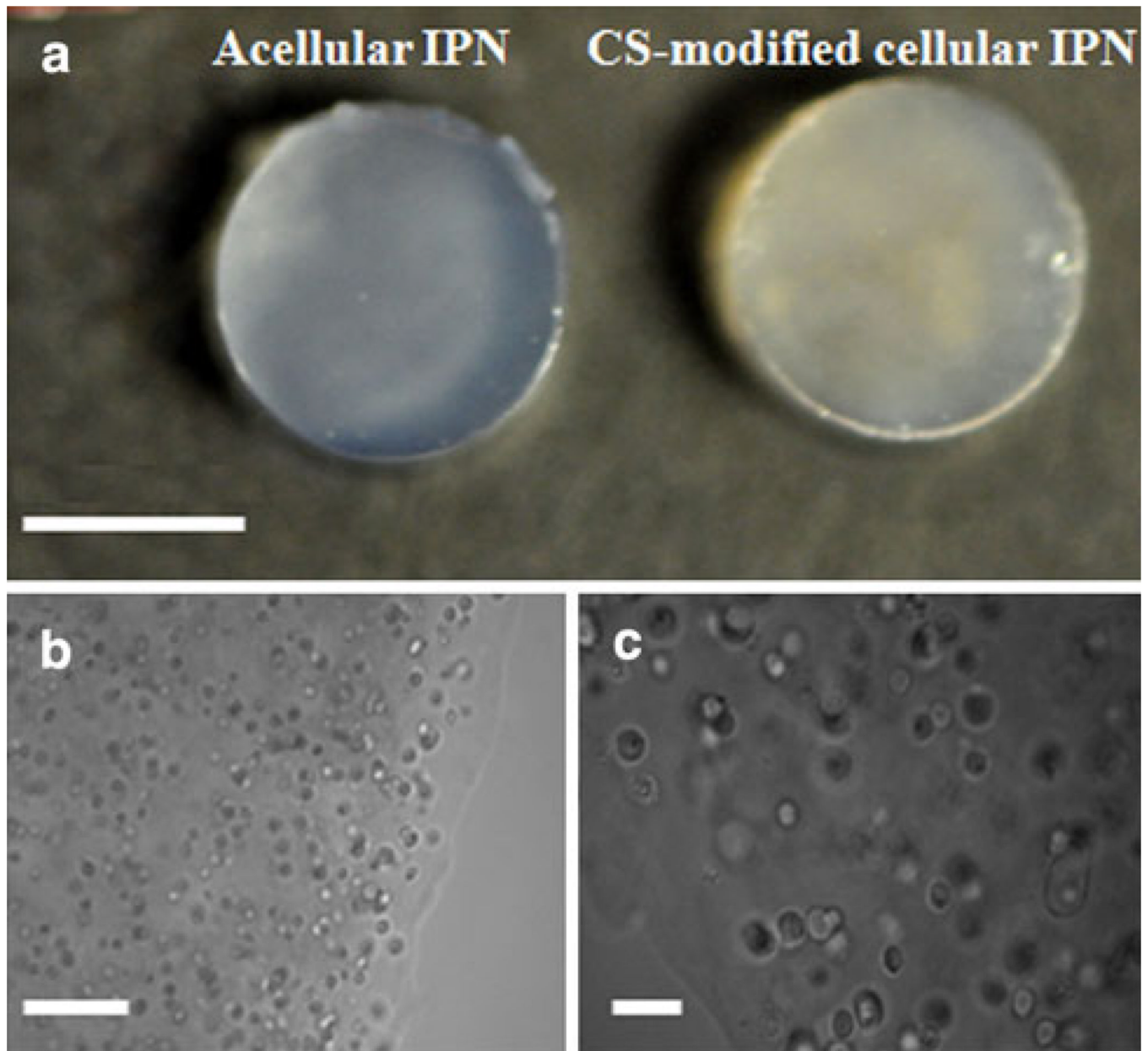


Fig. 5. Images of equilibrium-swollen IPN gels and encapsulated porcine chondrocytes: **a** an acellular IPN (*left*) gel and cellular CS modified IPN gel (*right*); **b** dispersed encapsulated chondrocyte in the IPN gel, $\times 100$; **c** their round morphology, $\times 200$. Bars: **a** 3 mm; **b** 100 μm ; **c** 50 μm

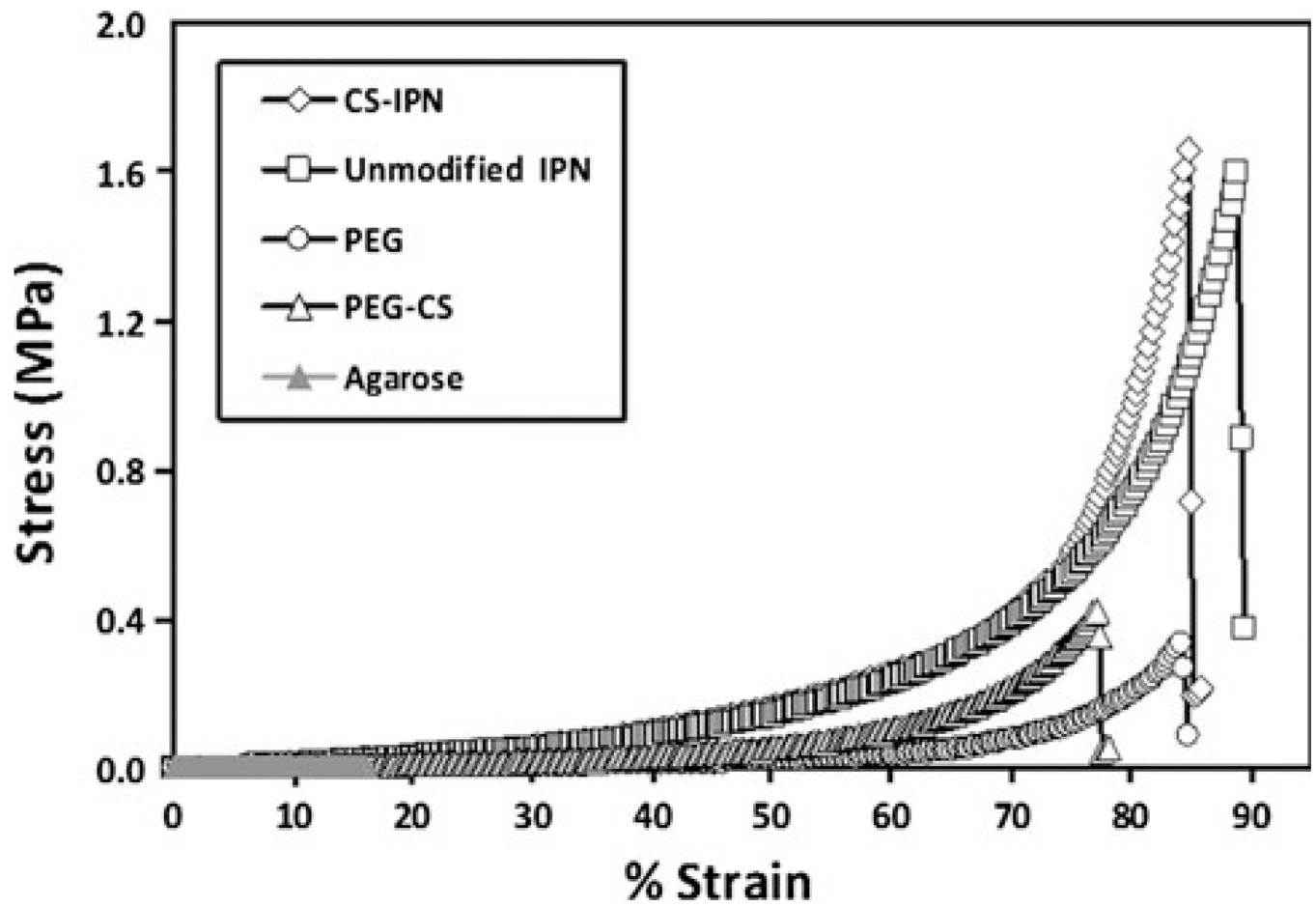


Fig. 6. Representative strain–stress curves for fully swollen hydrogel samples. Samples were compressed at a rate of 0.0005 mm/s until failure

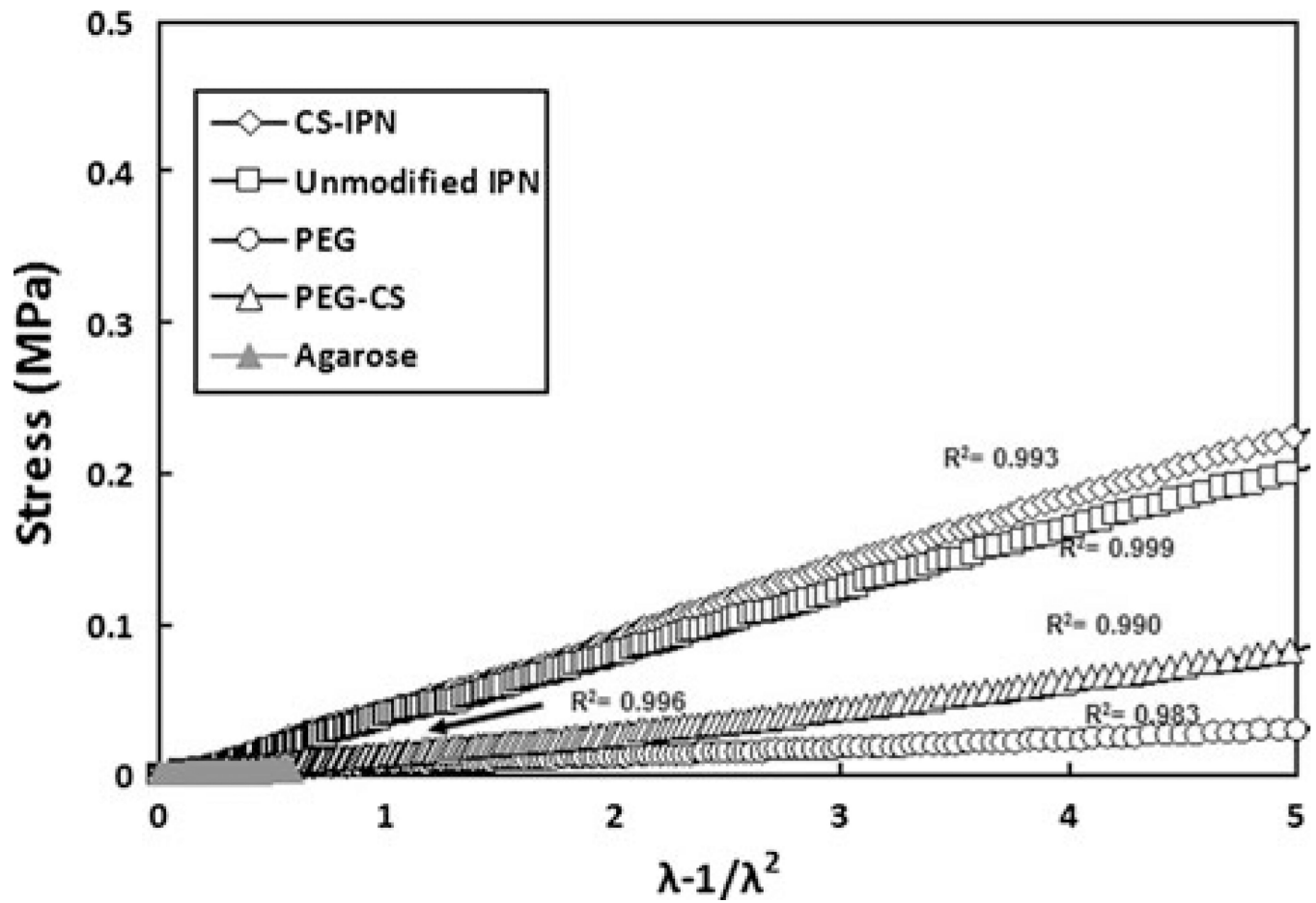


Fig. 7. Representative neo-Hookean elasticity model plots of stress versus strain function ($\lambda - 1/\lambda^2$), where $\lambda = L/L_0$. The slope of this plot is equal to the shear modulus (G)

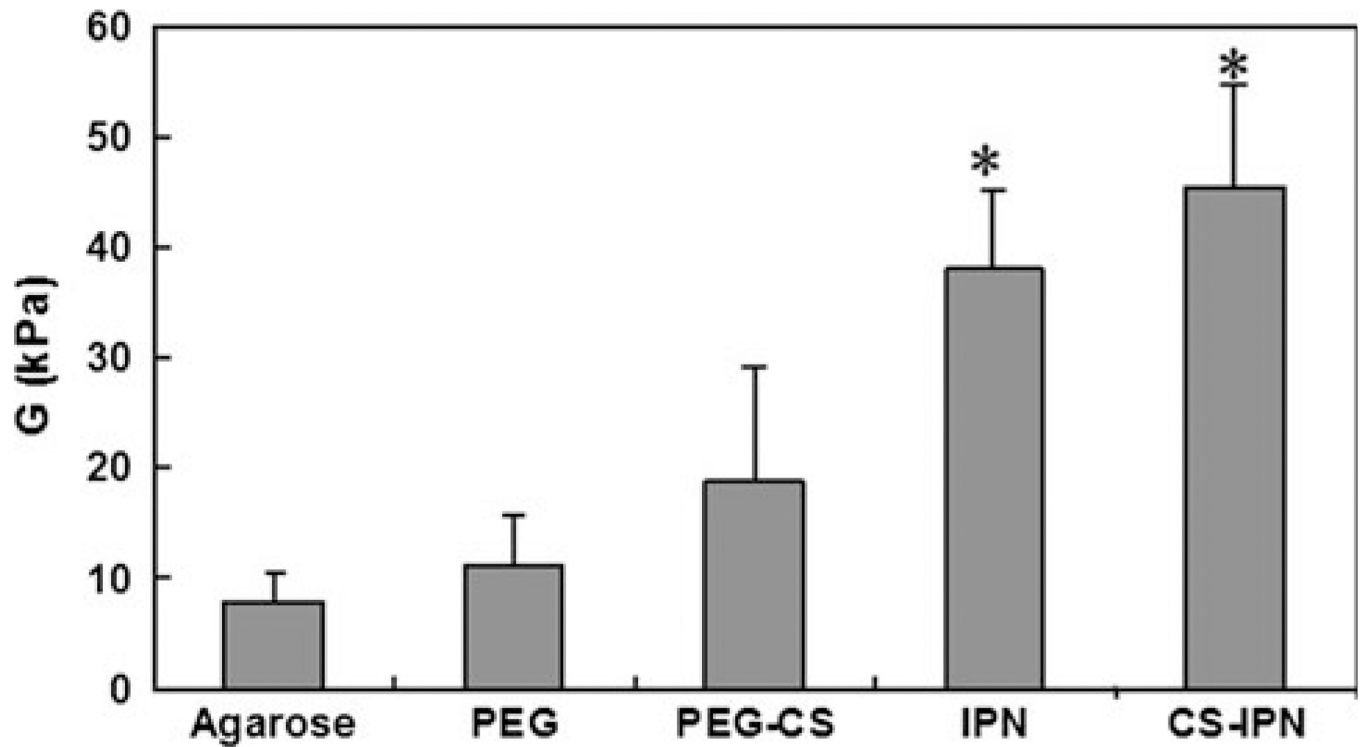


Fig. 8. Comparison of the compressive shear moduli, G (mean \pm standard deviation; $n = 5$ for all groups). *Values statistically significant from Agarose, PEG and PEG-CS groups (* $P < 0.05$). *PEG* poly(ethylene glycol), *PEG-CS* chondroitin sul-fate-poly(ethylene glycol) copolymer network, *IPN* interpenetrating network, *CS-IPN* chondroitin sulfate incorporated interpenetrating network

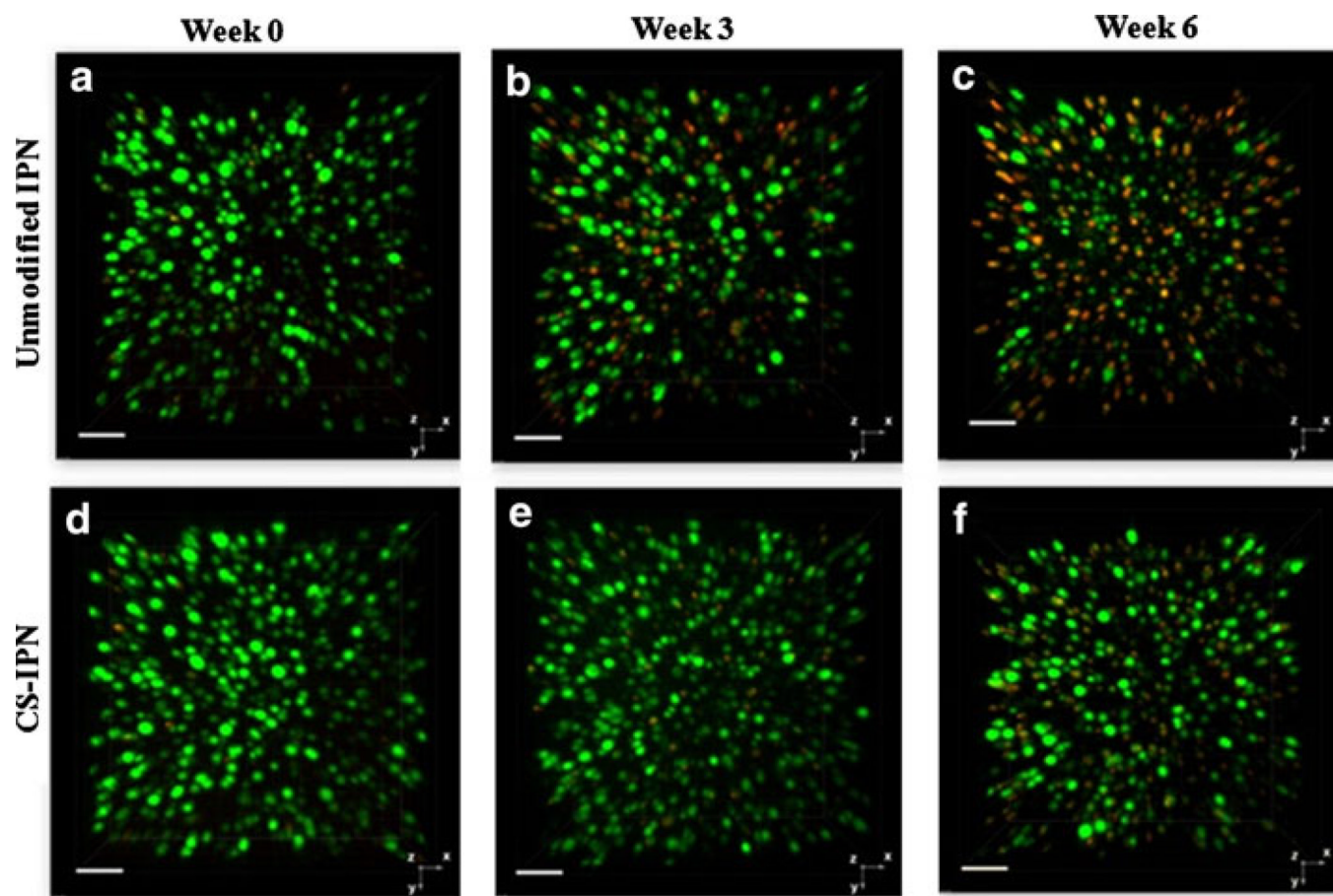


Fig. 9. 3-D Live/dead images of encapsulated chondrocytes in unmodified IPN gels **a–c** at the week 0, 3, and 6 culture period, respectively, and in CSincorporated IPN gels **d–f** at 0, 3, and 6 weeks, respectively. Hydrogel construct containing live cells labeled with Calcein AM (*green*) and dead cells labeled with ethidium homodimer-1 (*red*). Scale bar 50 μm (Color figure online)

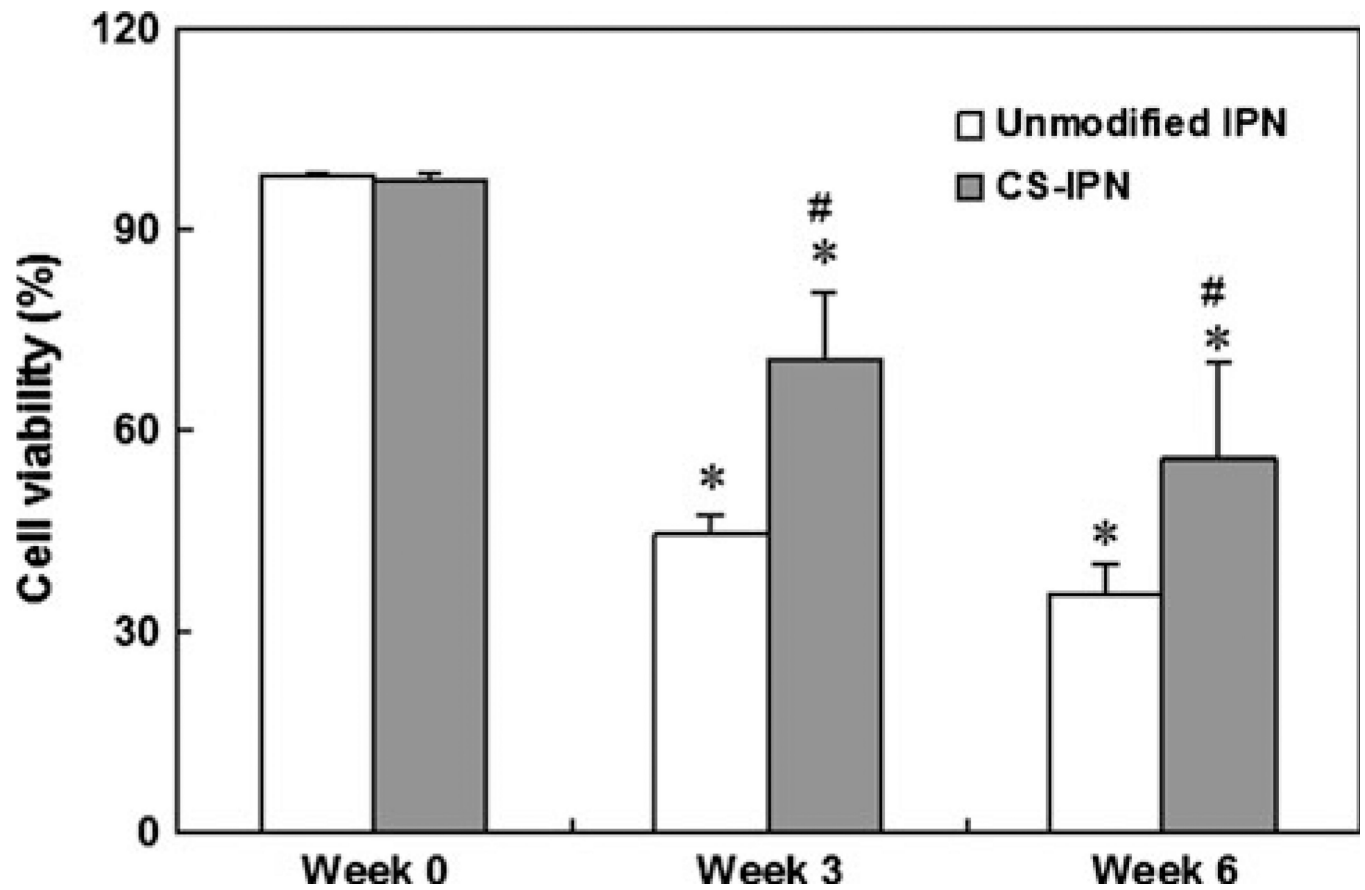


Fig. 10. Percent cell viability of encapsulated chondrocytes by image analysis mask statistics. Multiple confocal Z-scan series were performed on a representative sample in each group (mean \pm standard deviation). *Values statistically significant from week 0, while a #values statistically significant from other groups at that time ($P < 0.05$ and $n = 3$)

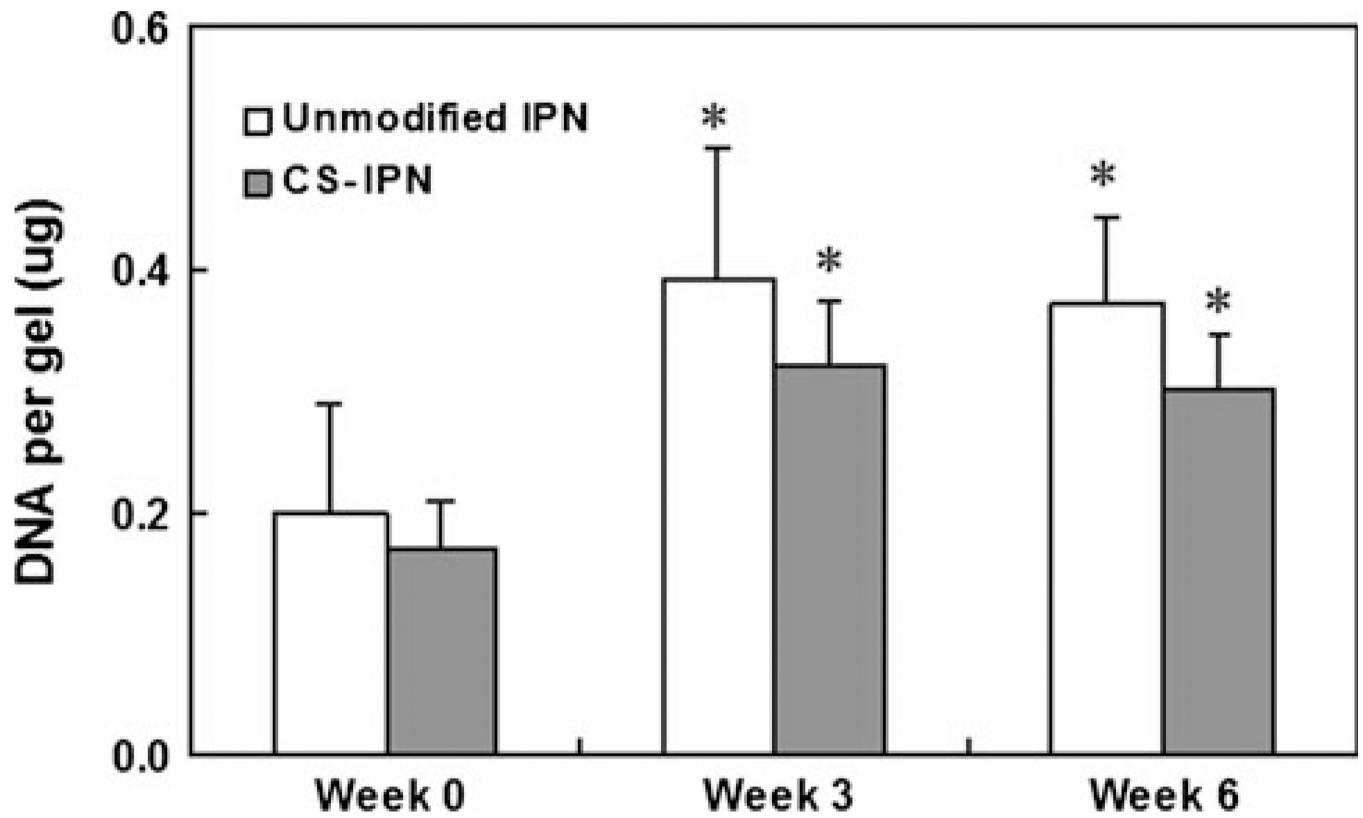


Fig. 11. Total DNA content within unmodified and CS-incorporated IPN gels at 0, 3, and 6 weeks. Values represent mean \pm standard deviation with $n = 4$. *Values statistically significant from week 0 ($P < 0.05$)

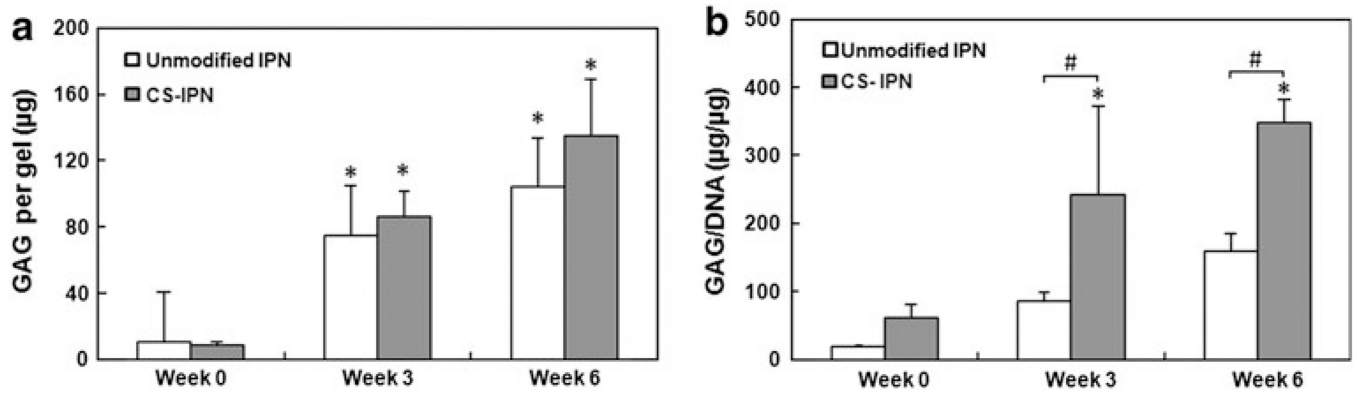


Fig. 12.

a Total GAG accumulated per gel (construct) within each unmodified IPN and CS-incorporated IPN gels with encapsulated chondrocytes at 0, 3, and 6 weeks. **b** For each gel groups, the total GAG accumulated were normalized to DNA content. Values represent mean \pm standard deviation with $n = 4$. *Values statistically significant from week 0 time point ($P < 0.05$), #statistically significant differences between the groups at that time point ($P < 0.05$). GAG glycosaminoglycan. Note that the GAG content associated with incorporated CS (averaging approximately 4–5 μg per construct) was subtracted from the actual GAG value to provide the values reported here

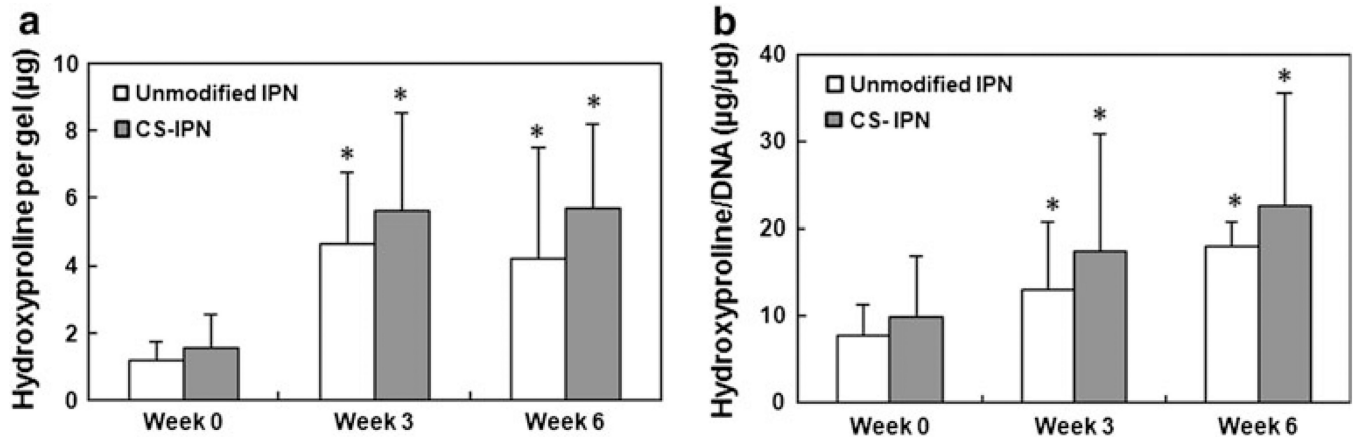


Fig. 13.

a Total collagen accumulated per gel (construct) within each unmodified IPN and CS-incorporated IPN gels with encapsulated chondrocytes at 0, 3, and 6 weeks. **b** For each gel groups, the total collagen accumulated were normalized to DNA content. *Error bars* represent mean \pm standard deviation with $n = 4$. Normalized collagen content increased significantly over the culture time, but this normalized collagen content was not statistically different between the groups at that time. *Values statistically significant from week 0 ($P < 0.05$)

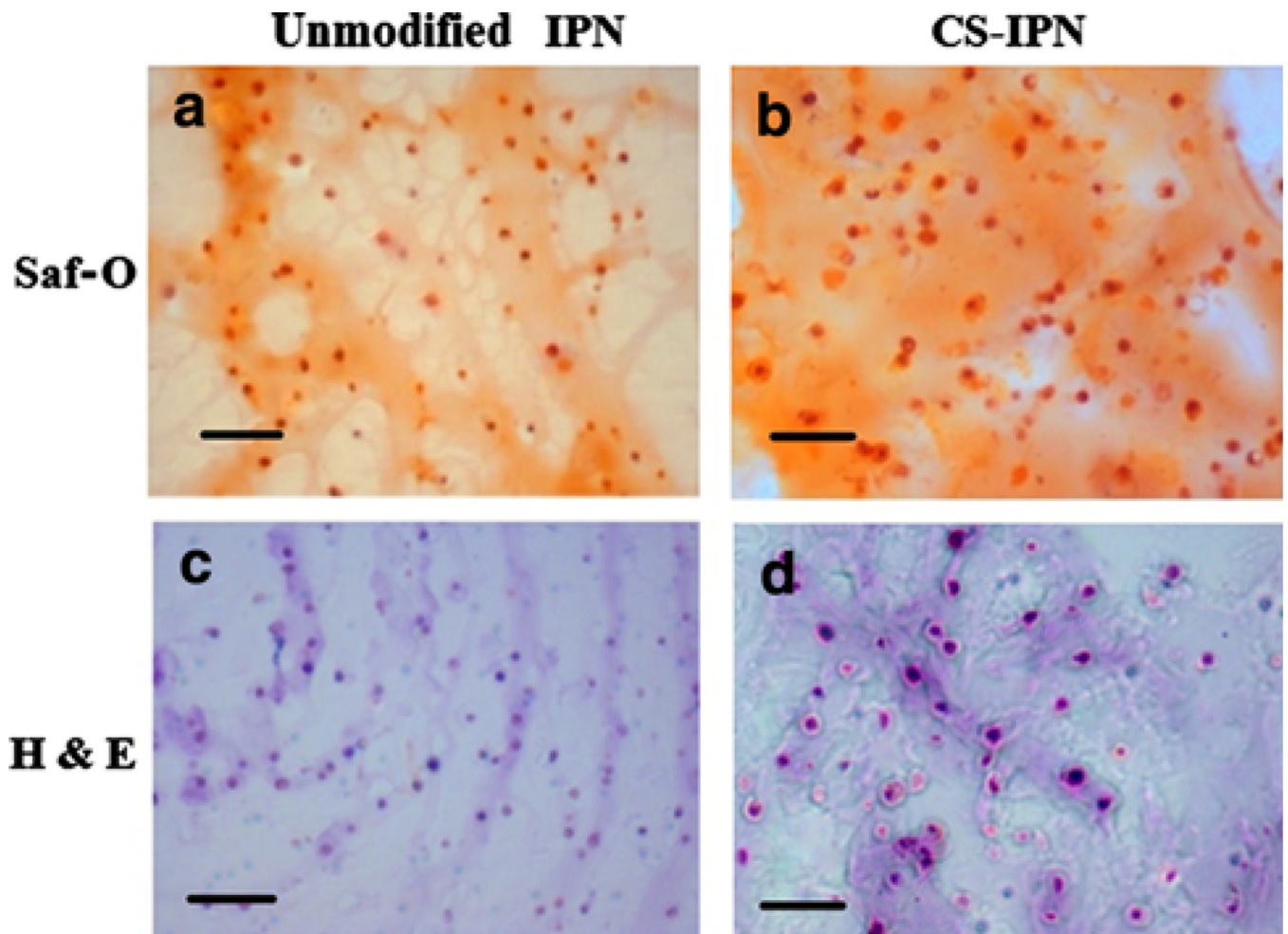


Fig. 14. Photomicrographs showing histological cross sections of IPN constructs after 6 weeks (original magnification $\times 100$ for all images). Sections stained with Safranin O (Saf-O) demonstrated GAG staining in a region of cartilage-like tissue in **a** the unmodified IPN and **b** the CS-incorporated IPN, while sections stained with H & E demonstrated pericellular matrix accumulation in **c** unmodified IPN and **d** CS-incorporated IPN gels. *Scale bar* 50 μm

Table 1

Mechanical and swelling properties of different gels

| Gel type | Compressive shear moduli G (kPa) ^{a,b,c} | Compressive elastic moduli E (kPa) ^{a,b,c} | E/G | Fracture stress (kPa) ^{c,e,f} | Fracture strain (%) ^d | Toughness (kJ/m ³) ^{c,e,f} | Total solid (%) ^d | Swelling degree Q |
|----------|---|---|-----------|--|----------------------------------|---|------------------------------|---------------------|
| Agarose | 7.8 ± 2.5 | 30 ± 13 | 3.8 ± 0.6 | ~3.2 | ~18 | ~0.2 | 2.4 ± 0.1 | 43.1 ± 5.7 |
| PEG | 10.2 ± 4.6 | 41 ± 25 | 4.0 ± 0.4 | 368 ± 289 | 82 ± 27 | 36 ± 19 | 7.3 ± 0.9 | 13.5 ± 2.5 |
| PEG-CS | 18.8 ± 8.9 | 60 ± 31 | 3.3 ± 0.8 | 395 ± 301 | 76 ± 21 | 54 ± 22 | 6.9 ± 0.2 | 15.0 ± 1.3 |
| IPN | 37.9 ± 9.3 | 136 ± 47 | 3.6 ± 0.9 | 935 ± 765 | 89 ± 34 | 116 ± 77 | 9.5 ± 0.2 | 11.0 ± 3.3 |
| CS-IPN | 45.4 ± 7.5 | 154 ± 34 | 3.3 ± 0.7 | 1036 ± 890 | 80 ± 25 | 127 ± 93 | 8.8 ± 0.8 | 12.6 ± 1.9 |

All values are reported as mean ± deviation, $n = 5$

G shear modulus, E Young's modulus, Q swelling degree, IPN : interpenetrating network, PEG : poly(ethylene glycol), $PEG-CS$: poly(ethylene glycol)-chondroitin sulfate copolymer network, $CS-IPN$: chondroitin sulfate incorporated interpenetrating network

^a IPN and CS-IPN were significantly different from agarose and PEG ($P < 0.05$)

^b IPN and CS-IPN were not statistically significantly different from agarose and PEG-CS

^c IPN was not statistically significantly different from CS-IPN

^d No statistical significance among PEG, PEG-CS, IPN, and CS-IPN groups

^e No statistical significance among PEG, PEG-CS, and IPN groups

^f CS-IPN were significantly different from agarose, PEG and PEG-CS groups ($P < 0.05$)